Physics Letters B 697 (2011) 477–481

Contents lists available at ScienceDirect

Physics Letters B

www.elsevier.com/locate/physletb

Importance of nuclear effects in the measurement of neutrino oscillation parameters

Enrique Fernandez Martinez [a,b,*], Davide Meloni [c]

[a] Max-Planck-Institut für Physik (Werner-Heisenberg-Institut), Föhringer Ring 6, 80805 München, Germany
[b] CERN, PH-TH Division, CH-1211 Genève 23, Switzerland
[c] Institut für Theoretische Physik und Astrophysik, Universität Würzburg, D-97074 Würzburg, Germany

ARTICLE INFO

Article history:
Received 29 November 2010
Received in revised form 2 February 2011
Accepted 16 February 2011
Available online 19 February 2011
Editor: A. Ringwald

Keywords:
Neutrino oscillations
Neutrino cross sections
Beta-beams

ABSTRACT

We investigate how models for neutrino–nucleus cross sections based on different assumptions for the nuclear dynamics affect the forecasted sensitivities to neutrino oscillation parameters at future neutrino facilities. We limit ourselves to the quasi-elastic regime, where the neutrino cross sections can be evaluated with less uncertainties, and discuss the sensitivity reach to θ_{13} and δ at a prototype low-γ β-beam, mostly sensitive to the quasi-elastic regime.

1. Introduction

In recent years the experimental study of neutrino oscillations has much contributed to our knowledge of particle physics by establishing non-vanishing neutrino masses and by measuring or constraining the corresponding mixing angles. Within the domain of neutrino oscillations, the main goal of the next generation of facilities is the measurement of the mixing angle θ_{13}, which at present is only limited by an upper bound, and the observation of leptonic CP violation, for which we have no hints at the moment. These measurements are extremely challenging, since the smallness of the present bound on $\sin\theta_{13} < 0.22$ at 3σ [1] constrains the signals to be very subleading. It is therefore necessary to have a good knowledge of the detector response function as well as an accurate knowledge of the beam to control the various systematic errors with a very good precision. For this task, novel ν beams with extremely low backgrounds and systematic uncertainties have been proposed for future measurements based on the decay of muons (neutrino factories [2,3]) or β-unstable ions (β-beams [4]). The ν_e fluxes from such decays would be extremely pure and the systematic errors very small, especially if the flux is normalized through a measurement with a near detector. Conversely, the systematic uncertainties associated with the detection process should be kept at the same accuracy level. It is usually argued that the ν_μ/ν_e neutrino–nucleus cross section ratio can be understood at the level of some percent and that the ν_e cross section can be measured with similar precision at a near detector so that the ν_μ signal can have systematic uncertainties of the order of a few percent at the far detector. This, however, does not take into account our present ignorance of the actual value of the cross section at low energies and how different models lead to forecasted sensitivities to the unknown parameters that differ by much larger margins than the few percent uncertainty normally considered. This question can severely impact the comparison of the relative performance of different facilities depending on the model adopted to parametrize their cross sections, particularly if the different facilities are sensitive to distinct energy regions. In this Letter we want to discuss more in detail this question showing that, when a realistic model of nuclear dynamics is adopted, the neutrino cross section can sizably affect the forecasted precision measurement of θ_{13} and the CP violating phase δ. It is beyond the scope of this Letter to discuss (and critically revise) all possible models for neutrino interactions, so we restrict ourselves to the Relativistic Fermi Gas (RFG) model, variants of which are widely used in many Monte Carlo codes and, as examples of more refined calculations, to the one based on the Spectral Function (SF) approach, on the Relativistic Mean Field (RMF) approximation and on the Random Phase Approximation (RPA), also including the effects of multinucleon contributions. The main features of these models are briefly summarized in Section 2 whereas in Section 3 we show how the measurement of θ_{13} and δ can be affected by the differ-

* Corresponding author at: CERN, PH-TH Division, CH-1211 Genève 23, Switzerland.
E-mail addresses: enrique.fernandez.martinez@cern.ch (E. Fernandez Martinez), davide.meloni@physik.uni-wuerzburg.de (D. Meloni).

0370-2693 © 2011 Elsevier B.V. Open access under CC BY license.
doi:10.1016/j.physletb.2011.02.043

ent descriptions of the nuclear dynamics. We draw our conclusions in Section 4.

2. Summary of the charged current neutrino–nucleus cross sections

We work in the Quasi-Elastic (QE) regime, which is of interest in many current and planned experiments (among them, MiniBooNE has already released its first cross section measurement [5]). The doubly-differential cross section, in which a neutrino carrying initial four-momentum $k = (E_\nu, \mathbf{k})$ scatters off a nuclear target to a state of four-momentum $k' = (E_\ell, \mathbf{k}')$ can be written in Born approximation as follows:

$$\frac{d^2\sigma}{d\Omega\, dE_\ell} = \frac{G_F^2 V_{ud}^2}{16\pi^2}\frac{|\mathbf{k}'|}{|\mathbf{k}|} L_{\mu\nu} W_A^{\mu\nu}, \tag{1}$$

where G_F is the Fermi constant and V_{ud} is the CKM matrix element coupling u and d quarks. The leptonic tensor, that can be written in the form

$$L_{\mu\nu} = 8\left[k'_\mu k_\nu + k'_\nu k_\mu - g_{\mu\nu}(k\cdot k') - i\varepsilon_{\mu\nu\alpha\beta}k'^{\beta}k^{\alpha}\right] \tag{2}$$

is completely determined by lepton kinematics, whereas the nuclear tensor $W_A^{\mu\nu}$, containing all the information on strong interactions dynamics, describes the response of the target nucleus. Its definition involves the initial and final hadronic states $|0\rangle$ and $|X\rangle$, carrying four momenta p_0 and p_X, respectively, as well as the nuclear electroweak current operator J_A^μ:

$$W_A^{\mu\nu} = \sum_X \langle 0|J_A^{\mu\dagger}|X\rangle\langle X|J_A^\nu|0\rangle \delta^{(4)}(p_0 + q - p_X), \tag{3}$$

where the sum includes all hadronic final states. The calculation of $W_A^{\mu\nu}$ is a complicated task which deserves some approximation; quite often the Impulse Approximation (IA) scheme is adopted, based on the assumptions that at large enough $\mathbf{q}$ the target nucleus is seen by the probe as a collection of individual nucleons and that the particles produced at the interaction vertex and the recoiling $(A-1)$-nucleon system evolve independently. Within this picture, the nuclear current can be written as a sum of one-body currents, i.e. $J_A^\mu \to \sum_i J_i^\mu$, while the final state reduces to the direct product of the hadronic state produced at the weak vertex (with momentum $\mathbf{p}'$) and that describing the $(A-1)$-nucleon residual system, with momentum $\mathbf{p}_\mathcal{R}$: $|X\rangle \to |i, \mathbf{p}'\rangle \otimes |\mathcal{R}, \mathbf{p}_\mathcal{R}\rangle$.

2.1. The spectral function approach

The calculation of the weak tensor as described in Ref. [6] naturally leads to the concept of spectral function. In fact, the final expression of the hadronic tensor can be cast in the following form:

$$W_A^{\mu\nu} = \frac{1}{2}\int d^3p\, dE\, P(\mathbf{p}, E)\frac{1}{4E_{|\mathbf{p}|}E_{|\mathbf{p}+\mathbf{q}|}} W^{\mu\nu}(\tilde{p}, \tilde{q}), \tag{4}$$

where $E_\mathbf{p} = \sqrt{|\mathbf{p}|^2 + m_N^2}$ and the function $P(\mathbf{p}, E)$ is the target *spectral function*, i.e. the probability distribution of finding a nucleon with momentum $\mathbf{p}$ and removal energy E in the target nucleus. It then encodes all the informations about the initial (struck) particle. The quantity $W^{\mu\nu}$ is the tensor describing the weak interactions of the i-th nucleon in free space; the effect of nuclear binding of the struck nucleon is accounted for by the replacement $q = (\nu, \mathbf{q}) \to \tilde{q} = (\tilde{\nu}, \mathbf{q})$ with $\tilde{\nu} = E_{|\mathbf{p}+\mathbf{q}|} - E_{|\mathbf{p}|}$. It follows that the second argument in the hadronic tensor is $\tilde{p} = (E_{|\mathbf{p}|}, \mathbf{p})$. Substituting Eq. (4) into Eq. (1), we get the final formula for the *nuclear* cross section:

$$\frac{d^2\sigma_{IA}}{d\Omega\, dE_\ell} = \int d^3p\, dE\, P(\mathbf{p}, E)\frac{d^2\sigma_{\text{elem}}}{d\Omega\, dE_\ell}, \tag{5}$$

in which we have redefined the *elementary* cross section as

$$\frac{d^2\sigma_{\text{elem}}}{d\Omega\, dE_\ell} = \frac{G_F^2 V_{ud}^2}{32\pi^2}\frac{|\mathbf{k}'|}{|\mathbf{k}|}\frac{1}{4E_\mathbf{p}E_{|\mathbf{p}+\mathbf{q}|}} L_{\mu\nu}W^{\mu\nu}. \tag{6}$$

The calculation of $P(\mathbf{p}, E)$ has been only carried out for $A \leqslant 4$ [7]; however, thanks to the simplifications associated with translation invariance, highly accurate results are also available for uniform nuclear matter, i.e. in the limit $A \to \infty$ with $Z = A/2$ [8] (Z denotes the number of protons). The spectral functions for medium-heavy nuclei have been modeled using the Local Density Approximation (LDA) [9], in which the experimental information obtained from nucleon knock-out measurements is combined with the results of theoretical calculations of the nuclear matter $P(\mathbf{p}, E)$ at different densities.

2.2. The relativistic Fermi gas

The RFG [10] model, widely used in Monte Carlo simulations, provides the simplest form of the spectral function:

$$P_{RFGM}(\mathbf{p}, E) = \left(\frac{6\pi^2 A}{p_F^3}\right)\theta(p_F - \mathbf{p})\delta(E_\mathbf{p} - E_B + E), \tag{7}$$

where p_F is the Fermi momentum and E_B is the average binding energy, introduced to account for nuclear binding. The term in parenthesis is a constant needed to normalize the spectral function to the number of target nucleons, A. Thus, in this model p_F and E_B are two parameters that are *adjusted* to reproduce the experimental data. For oxygen, the analysis of electron scattering data yields $p_F = 225$ MeV and $E_B = 25$ MeV [11].

2.3. The relativistic mean field approach

Within the RMF approximation we refer to the model described in [12], where, like in the previous cases, the nuclear current is written as a sum of single-nucleon currents. The wave functions for the target and the residual nuclei are described in terms of an independent-particle model. Then, the transition matrix elements can be cast in the following form:

$$J_N^\mu(\omega, \vec{q}) = \int d\vec{p}\, \bar{\psi}_F(\vec{p} + \vec{q})\hat{J}_N^\mu(\omega, \vec{q})\psi_B(\vec{p}), \tag{8}$$

where ψ_B and ψ_F are the wave functions for initial bound and final outgoing nucleons, respectively, and $\hat{J}_N^\mu$ is the relativistic current operator. In particular, the relativistic bound-state wave functions (for both initial and outgoing nucleons) are obtained as a solution of the Dirac equation, in the presence of the same relativistic nuclear mean field potential, derived from a Lagrangian containing σ, ω and ρ mesons. The calculated cross sections correctly account for the inclusive cross section which are interested in.

2.4. The random phase approximation

The last model we want to take into account has been introduced in [14], where the hadronic tensor is expressed in terms of the nuclear response functions treated in the Random Phase Approximation (RPA). The response functions are related to the imaginary part of the corresponding full polarization propagators and the introduction of the RPA approximation means that the polarization propagators are the solutions of integral equations

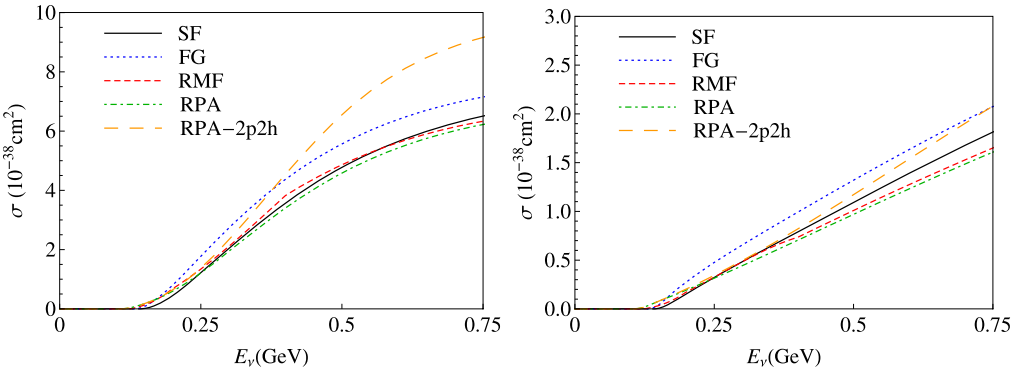

Fig. 1. Total charged current QE cross sections for the $\nu_\mu\,^{16}O \to \mu^- X$ (left panel) and $\bar{\nu}_\mu\,^{16}O \to \mu^+ X$ (right panel) processes in the energy range $E_\nu \sim [0, 0.75]$ GeV.

involving the bare propagators and the effective interaction between particle–hole excitations. Within this formalism, the authors of [14] were able to show that multinucleon terms sizably increase the genuine charged current QE cross section [14,15] in such a way to reproduce the MiniBooNE results [5]. The mechanism responsible for the enhancement that brings the theoretical cross section into agreement with the data is multi nucleon knock out, leading to two particle–two hole (2p2h) nuclear final states. In the following, we will refer to this "generalized" QE cross section as RPA-2p2h whereas we adopt the short RPA for the genuine QE cross section.

2.5. Comparison of the cross sections

To summarize this section, we present in Fig. 1 a comparison of the five total QE cross sections for the $\nu_\mu\,^{16}O \to \mu^- X$ process (left panel) and $\bar{\nu}_\mu\,^{16}O \to \mu^+ X$ (right panel), in the energy range $E_\nu \sim [0, 0.75]$ GeV. The curves have been computed using the dipole structure of the form factors and, in particular, a value of the axial mass close to $m_A \sim 1$ GeV. As it can be easily seen in the left panel, the RFG prediction sizably overestimates the SF, RMF and RPA results by roughly 15%, a fact that is well known to happen also for many other models with a more accurate description of the nuclear dynamics than the RFG approach (see, for instance, [13]). On the other hand, the inclusion of 2p2h contributions largely enhances the QE cross section in the RPA approximation for energies above ∼0.5 GeV, although it is smaller than the RFG at smaller energies. For antineutrinos (right panel) the observed pattern is almost the same. From this comparison, a *qualitative* understanding of the impact of different models of neutrino–nucleus cross sections on the forecasted sensitivity of future facilities can be already derived. A *quantitative* analysis of these effects will be the subject of the next section.

3. The impact on the (θ_{13}–δ) measurement

To estimate the impact of different models of the cross section on the measurement of θ_{13} and leptonic CP violation we choose a $\gamma = 100$ β-beam facility as a representative example. The choice is motivated because the neutrino flux from such a facility spans up to ∼0.7 GeV with the peak around 0.3 GeV and is thus mostly sensitive to the quasi-elastic region explored here. The β-beam concept was first introduced in Ref. [4] and involves the production of β-unstable ions, accelerating them to some reference energy, and allowing them to decay in the straight section of a storage ring, resulting in a very intense and pure ν_e or $\bar{\nu}_e$ beams. The $\nu_e \to \nu_\mu$ "golden channel", which has been identified as the most sensitive to all the unknown parameters [17], can be probed at a far detector. We have considered here the original β-beam proposal, where ^{18}Ne (^{6}He) ions are accelerated to $\gamma \sim 100$ at the CERN SPS and stored so that ν_e ($\bar{\nu}_e$) beams are produced and the golden channel oscillation is searched for at a Mton class water Cerenkov detector located at $L = 130$ km at the Frejus site, detailed analyses of the physics performance of this setup can be found in Refs. [18–27]. In order to simulate the detector response when exposed to such a beam both in terms of signal efficiency and background, we have used the migration matrices derived in Ref. [28]. Systematic errors of 2.5% and 5% in the signal and background respectively have been taken into account. In all the simulations the following best fit values and 1σ errors for the known oscillation parameters were assumed [1] $\Delta m^2_{21} = (7.6 \pm 0.2) \cdot 10^{-5}$ eV^2, $\Delta m^2_{31} = (2.5 \pm 0.1) \cdot 10^{-3}$ eV^2, $\theta_{12} = 34.0 \pm 1.0$ and $\theta_{23} = 45.0 \pm 3.6$. These parameters were marginalized over to present the final curves. The evaluation of the performance of the facility made use of the GLoBES software [29,30]. It is important to notice that we are only using the quasi-elastic contribution to the neutrino cross section depicted in Fig. 1.

As an illustration we have focused on the dependence on the nuclear model adopted of two different observables, namely the *CP and θ_{13} discovery potentials*, defined as the values of the CP-violating phase δ_{CP} and θ_{13} for which respectively the hypothesis of CP conservation $\delta_{CP} = 0$, $\pm\pi$ or $\theta_{13} = 0$ can be excluded at 3σ after marginalizing over all other parameters. The CP discovery potential is shown in Fig. 2, where we superimposed the results obtained using the RFG cross section and the SF, RMF and RPA calculations. In the left panel, the CP discovery potential is represented in the $(\theta_{13}, \delta_{CP})$-plane; we clearly see that, for $\delta_{CP} \sim \pm 90°$ (where the sensitivity is maximal) the RFG model gives a prediction which is around a factor 2 better than the SF, RMF and RPA models (which, as expected, behave almost in the same way) in $\sin^2 2\theta_{13}$ and around a 40% better than the RPA-2p2h. This is not surprising because the β-beam facility used in our simulations mainly probes energies smaller than 0.5 GeV, where the RFG is still larger than any other model (see Fig. 1). For the other points in the parameter space, the difference is less evident but still significant. The same information can be summarized in the right panel making use of the δ *fraction* (δ_F), that represents the fraction of values of δ_{CP} for which CP can be discovered at a given θ_{13}. The δ fraction has a maximum around $\sin^2 2\theta_{13} \sim 10^{-2}$ where the RFG model predicts $\delta_F \sim 0.75$ and the other models give $\delta_F \sim 0.7$. The difference in the sensitivity to θ_{13} can be seen in Fig. 3 where we show the results in the $(\sin^2 2\theta_{13}, \delta_{CP})$-plane. In this case the predictions of the SF, RMF and RPA models differ by up to a factor of ∼60% compared to the RFG model for $\delta_{CP} \sim \pm 90°$ while the difference is less pronounced for $\delta_{CP} \sim 0°$. The RPA-2p2h results are

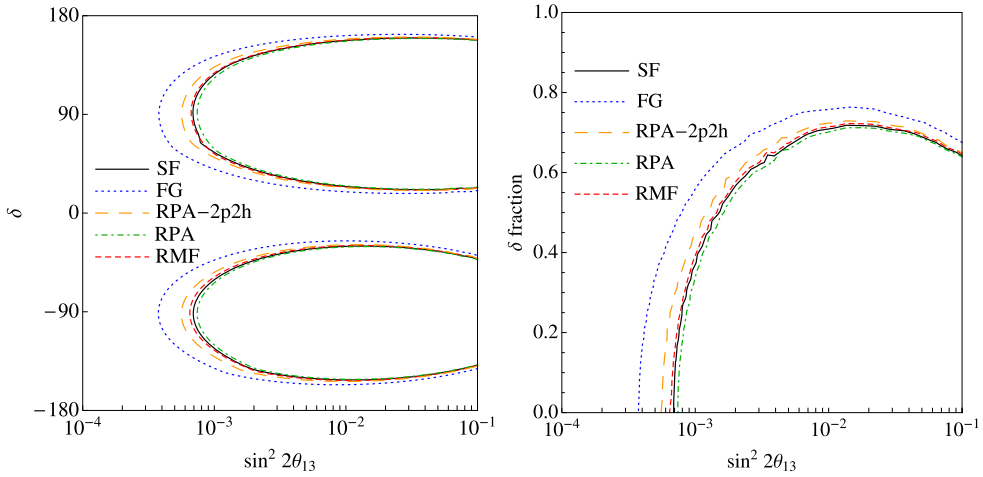

Fig. 2. Left panel: CP discovery potential in the $(\theta_{13}, \delta_{CP})$-plane. Solid lines refer to the SF model, dotted lines to the RFG, short-dashed lines to the RMF, dot-dashed to RPA and long-dashed to RPA-2p2h. Right panel: the CP fraction.

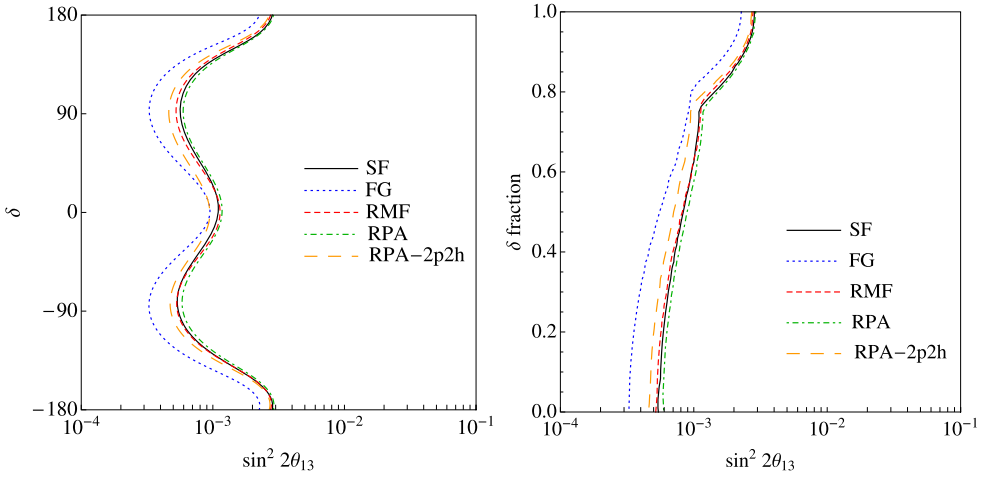

Fig. 3. Left panel: θ_{13} discovery potential in the $(\theta_{13}, \delta_{CP})$-plane. Solid lines refer to the SF model, dotted lines to the RFG, short-dashed lines to the RMF, dot-dashed to RPA and long-dashed to RPA-2p2h. Right panel: the CP fraction.

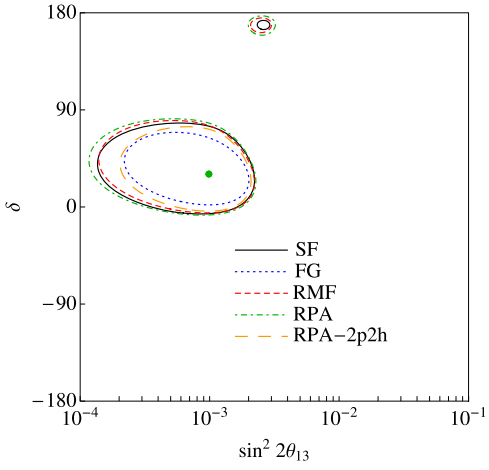

Fig. 4. 90% CL contour for the input value $(\theta_{13}, \delta_{CP}) = (0.9°, 30°)$. Solid lines refer to the SF model, dotted lines to the RFG, short-dashed lines to the RMF, dot-dashed to RPA and long-dashed to RPA-2p2h.

more similar to the RFG for $\delta_{CP} \sim 0°$ and to the other models for $\delta_{CP} \sim 180°$. This is also evident in the right panel where we show the CP fraction.

Finally, it is interesting to observe the effect of using different nuclear models also in the simultaneous determination of θ_{13} and δ_{CP}. We present an example in Fig. 4 where, for the input value $(\theta_{13}, \delta_{CP}) = (0.9°, 30°)$, indicated with a dot, we show the capability of the β-beam to reconstruct the true values of our observables at 90% CL. For the sake of simplicity, we did not include degenerate solutions coming from our ignorance of the octant of θ_{23} and the hierarchy in the neutrino mass ordering but only the so-called "intrinsic" one. The main feature here is that using the RFG and RPA-2p2h models we are able to reconstruct the true values of θ_{13} and δ_{CP} within reasonable uncertainties, whereas with the other models we can only measure two distinct disconnected regions (the fake one around the value of θ_{13} and $\delta_{CP} \sim 180°$), which worsen the global sensitivity on those parameters. The effects we have mentioned have been generalized to account for the following cases:

- the value of the axial mass does not fill the gap among the SF approach and the RFG model, at least in the range $m_A \in [1, 1.2]$ GeV. This is not surprising and has been already the subject of an extensive analysis [16];
- the same sensitivity behavior as observed in Figs. 2–3 has been also seen for a different nuclear target, namely ^{56}Fe. This points to the conclusion that the RFG model overestimates

the sensitivities to θ_{13} and δ_{CP} for a vast class of nuclear targets.

4. Conclusion

In this Letter we have analyzed the impact of different neutrino–nucleus charged current QE cross sections on the forecasted sensitivity of the future neutrino facilities to the parameters θ_{13} and δ_{CP}. We considered five different calculations, based on the RFG model (widely used in the Monte Carlo codes) and those based on the SF approach, on the RMF approximation and on the RPA (including multinucleon contributions, also) in the quasi-elastic regime. We found that the sensitivities computed from SF, RMF and RPA (without the multinucleon contribution) models are worse than the RFG results, for both θ_{13} and δ_{CP}, by up to a factor 2 when an oxygen nuclear target is used to compute the event rates. To a less extent, this is also true for the RPA-2p2h model, due to the fact that the quasi-elastic cross section is larger than the genuine quasi-elastic cross section. These variations with the nuclear models are so large that they cannot be taken into account with the few percent systematic error uncertainty expected from dedicated measurements at near detectors. Indeed, the present uncertainty is much larger and allows for discrepancies between models that can strongly affect the forecasted sensitivity of a given facility, implying that special care must be adopted when comparing the performance of different facilities. We have also checked that other nuclear targets produce quantitatively similar results. This suggests that the use in Monte Carlo simulations of more refined nuclear models for the neutrino–nucleus interaction is mandatory, especially for those facilities whose bulk of events is in the quasi-elastic regime.

Acknowledgements

We are strongly indebted to Omar Benhar for providing us with the oxygen and iron spectral functions. We also want to thank Maria Barbaro, Juan Antonio Caballero and Jose Udias for providing the neutrino–nucleus cross sections for the RMF approach, Marco Martini for the cross sections in the RPA and Magda Ericson and Sergio Palomares Ruiz for useful comments on the manuscript. D.M. was supported by the Deutsche Forschungsgemeinschaft, contract WI 2639/2-1. E.F.M. was supported by theMax-Planck-Institut für Physik, where this study was commenced, and CERN, where it was finalized. E.F.M. also acknowledges support from the European Community under the European Commission Framework Programme 7 Design Study: EUROnu, Project Number 212372.

References

[1] M.C. Gonzalez-Garcia, M. Maltoni, Phys. Rep. 460 (2008) 1, arXiv:0704.1800 [hep-ph].
[2] S. Geer, Phys. Rev. D 57 (1998) 6989, arXiv:hep-ph/9712290;
S. Geer, Phys. Rev. D 59 (1999) 039903 (Erratum).
[3] A. De Rujula, M.B. Gavela, P. Hernandez, Nucl. Phys. B 547 (1999) 21, arXiv:hep-ph/9811390.
[4] P. Zucchelli, Phys. Lett. B 532 (2002) 166, arXiv:hep-ex/0107006.
[5] A.A. Aguilar-Arevalo, et al., MiniBooNE Collaboration, Phys. Rev. D 81 (2010) 092005, arXiv:1002.2680 [hep-ex].
[6] O. Benhar, N. Farina, H. Nakamura, M. Sakuda, R. Seki, Phys. Rev. D 72 (2005) 053005, arXiv:hep-ph/0506116;
O. Benhar, D. Meloni, Nucl. Phys. A 789 (2007) 379, arXiv:hep-ph/0610403.
[7] A.E.L. Dieperink, T. de Forest, I. Sick, Phys. Lett. B 63 (1976) 261;
C. Ciofi degli Atti, E. Pace, G. Salmè, Phys. Rev. C 21 (1980) 805;
H. Meier-Hajduk, Ch. Hadjuk, P.U. Sauer, Nucl. Phys. A 395 (1983) 332;
C. Ciofi degli Atti, S. Liuti, S. Simula, Phys. Rev. C 41 (1990) R2474;
H. Morita, T. Suzuki, Prog. Theor. Phys. 86 (1991) 671;
O. Benhar, V.R. Pandharipande, Phys. Rev. C 47 (1993) 2218.
[8] O. Benhar, A. Fabrocini, S. Fantoni, Nucl. Phys. A 505 (1989) 267;
A. Ramos, A. Polls, W.H. Dickhoff, Nucl. Phys. A 503 (1989) 1.
[9] O. Benhar, A. Fabrocini, S. Fantoni, I. Sick, Nucl. Phys. A 579 (1994) 493.
[10] R.A. Smith, E.J. Moniz, Nucl. Phys. B 43 (1972) 605;
R.A. Smith, E.J. Moniz, Nucl. Phys. B 101 (1975) 547 (Erratum);
E.J. Moniz, Phys. Rev. 184 (1969) 1154.
[11] E.J. Moniz, I. Sick, R.R. Whitney, J.R. Ficenec, R.D. Kephart, W.P. Trower, Phys. Rev. Lett. 26 (1971) 445.
[12] J.M. Udias, J.A. Caballero, E. Moya de Guerra, J.R. Vignote, A. Escuderos, Phys. Rev. C 64 (2001) 024614, arXiv:nucl-th/0101038;
C. Maieron, M.C. Martinez, J.A. Caballero, J.M. Udias, Phys. Rev. C 68 (2003) 048501, arXiv:nucl-th/0303075;
J.A. Caballero, J.E. Amaro, M.B. Barbaro, T.W. Donnelly, C. Maieron, J.M. Udias, Phys. Rev. Lett. 95 (2005) 252502, arXiv:nucl-th/0504040;
M.C. Martinez, P. Lava, N. Jachowicz, J. Ryckebusch, K. Vantournhout, J.M. Udias, Phys. Rev. C 73 (2006) 024607, arXiv:nucl-th/0505008.
[13] F. Sanchez, M. Sorel, L. Alvarez-Ruso (Eds.), Proceedings of the Sixth International Workshop on Neutrino–Nucleus Interactions in the Few-GeV Region (NUINT-09), AIP Conference Proceedings, vol. 1189, 2010.
[14] M. Martini, M. Ericson, G. Chanfray, J. Marteau, Phys. Rev. C 80 (2009) 065501, arXiv:0910.2622 [nucl-th].
[15] M. Martini, M. Ericson, G. Chanfray, J. Marteau, Phys. Rev. C 81 (2010) 045502, arXiv:1002.4538 [hep-ph].
[16] O. Benhar, D. Meloni, Phys. Rev. D 80 (2009) 073003, arXiv:0903.2329 [hep-ph].
[17] A. Cervera, A. Donini, M.B. Gavela, J.J. Gomez Cadenas, P. Hernandez, O. Mena, S. Rigolin, Nucl. Phys. B 579 (2000) 17, arXiv:hep-ph/0002108;
A. Cervera, A. Donini, M.B. Gavela, J.J. Gomez Cadenas, P. Hernandez, O. Mena, S. Rigolin, Nucl. Phys. B 593 (2001) 731 (Erratum).
[18] M. Mezzetto, J. Phys. G 29 (2003) 1771, arXiv:hep-ex/0302007.
[19] M. Mezzetto, Nucl. Phys. Proc. Suppl. 143 (2005) 309, arXiv:hep-ex/0410083.
[20] A. Donini, E. Fernandez-Martinez, P. Migliozzi, S. Rigolin, L. Scotto Lavina, Nucl. Phys. B 710 (2005) 402, arXiv:hep-ph/0406132.
[21] A. Donini, E. Fernandez-Martinez, S. Rigolin, Phys. Lett. B 621 (2005) 276, arXiv:hep-ph/0411402.
[22] A. Donini, D. Meloni, S. Rigolin, Eur. Phys. J. C 45 (2006) 73, arXiv:hep-ph/0506100.
[23] P. Huber, M. Lindner, M. Rolinec, W. Winter, Phys. Rev. D 73 (2006) 053002, arXiv:hep-ph/0506237.
[24] J.E. Campagne, M. Maltoni, M. Mezzetto, T. Schwetz, JHEP 0704 (2007) 003, arXiv:hep-ph/0603172.
[25] W. Winter, Phys. Rev. D 78 (2008) 037101, arXiv:0804.4000 [hep-ph].
[26] W. Winter, arXiv:0809.3890 [hep-ph].
[27] E. Fernandez-Martinez, Nucl. Phys. B 833 (2010) 96, arXiv:0912.3804 [hep-ph].
[28] J. Burguet-Castell, D. Casper, E. Couce, J.J. Gomez-Cadenas, P. Hernandez, Nucl. Phys. B 725 (2005) 306, arXiv:hep-ph/0503021.
[29] P. Huber, M. Lindner, W. Winter, Comput. Phys. Commun. 167 (2005) 195, arXiv:hep-ph/0407333.
[30] P. Huber, J. Kopp, M. Lindner, M. Rolinec, W. Winter, Comput. Phys. Commun. 177 (2007) 432, arXiv:hep-ph/0701187.